A simple method for demagnetizing large NdFeB permanent magnets

Bahl, Christian R.H.; Eder, Martin A.; Boland, Greg; Abrahamsen, Asger B.

Published in:
IEEE Transactions on Magnetics

Link to article, DOI:
10.1109/TMAG.2020.3002098

Publication date:
2020

Document Version
Peer reviewed version

A simple method for demagnetizing large NdFeB permanent magnets

Christian R.H. Bahl[1], Martin A. Eder[2], Greg Boland[1,3], Asger B. Abrahamsen[2]

[1]DTU Energy, Technical University of Denmark, Anker Engelunds Vej, DK-2800 Lyngby, Denmark
[2]DTU Wind Energy, Technical University of Denmark, Frederiksborgvej 399, DK-4000 Roskilde, Denmark
[3]Polytech Nantes, Rue Christian Pauc, 44300 Nantes, France

Prior to processing magnetic NdFeB material for recycling it must be demagnetised. Here we demonstrate a simple low-cost method. Large blocks of NdFeB permanent magnets of dimension 10 cm x 7 cm x 2 cm and with the easy axis along the shortest dimension, are shown to demagnetise when heated on a planar induction heating device. The initial magnetisation of the magnets is reduced by a factor of 10 within a period of 30 minutes, in which the surface temperature of the magnet reaches 225 °C. This method simplifies the demagnetisation process of the permanent magnets in wind turbine generators as part of the rapidly increasing demand for improved recycling capabilities of permanent magnets.

***Index Terms*— Permanent magnet, Recycling, Induction heating, Permanent magnet generators, Wind turbines.**

I. Introduction

Offshore wind turbine installations in Europe are expected to increase ten-fold in capacity during the next decade in order to reduce the greenhouse gas emissions as outlined in the 2015 Paris Agreement [1]. The technical advancements needed to reach the target are an increase of the turbine size to 10-15 MW as well as more cost efficient substructures [2]. The upscaling of wind turbine rotors entails larger drive trains, which have to comply with the reliability demand of the offshore environment. This has caused a division among the wind turbine manufactures in using a gearbox and a medium speed synchronous generator or a large ring shaped generator connected directly to the shaft of the turbine [3]. The gearbox drive train is considered compact and cost efficient, but has the downside that the gearbox is a wear-component, which is costly to replace at sea. The direct drive train is often more bulky and more expensive, but is expected to live up to the design lifetime of the turbine. A consequence of choosing a direct drive train is the torque rating of the generator and thereby the consumption of NdFeB magnets needed to generate the magnetic field inside the generator is increased compared to the medium speed generator. The typical consumption of NdFeB for a medium speed generator combined with a gearbox is about 70 kg/MW, whereas a direct drive generator needs about 700 kg/MW [4].

The capacity of new offshore turbines needed in Europe for the next decade is about 50-100 GW[1] and if half of those are based on direct drive technology then the total amount of NdFeB permanent magnets required will range between 19,000 and 39,000 tons. Considering an estimated price of 30 €/kg [5] emphasizes the demand of a vast amount of rather expensive material, where most of the world production is based in China. In order to ensure a steady supply of NdFeB magnets for the European wind energy industry it becomes increasingly important to develop recycling capabilities for NdFeB magnets from wind turbine generators that are either being scrapped or that are reaching End-Of-Life. The design life-time of offshore turbines is 25 years causing a time lag before the magnets become available for recycling. However, even scrapping of just a few wind turbine generators due to failures etc. would result in large quantities of available material, as a single 10 MW generator accommodates between 700 kg and 7 tons of NdFeB permanent magnets, depending on the type of drive train.

Recycling of NdFeB magnets into new magnets with similar properties was demonstrated by Zakotnik *et al.* using hydrogen decrepitating [6]. The work on recycling NdFeB is reviewed in refs. [7,8].

In any recycling process the demagnetization of the material is a prerequisite for safety and practical reasons. In the literature on recycling this crucial step is rarely addressed in sufficient detail. Most often, it is just stated that the material was heated to high temperature, which could be done using a non-magnetic furnace, the aim being to bring it above the Curie temperature (T_C) of about 573 K. The other alternative method is 'Degaussing', where a strong magnet field is oscillated at gradually decreasing amplitudes [9].

A method for scrapping a direct drive generator is to first separate the ring holding the NdFeB permanent magnets from the rest of the generator. Subsequently the magnets are heated up using a gas torch, while they are still sitting in their individual steel cassettes. Thereafter, the magnets are extracted by first cutting the steel cassettes open followed by manual detachment using a hammer [10].

This paper demonstrates a practical and fast method for demagnetizing large End-Of-Life NdFeB magnets obtained from a scrap merchant, with no information about their initial properties. It is demonstrated how a simple induction heater can be utilized to heat magnet blocks in a controlled and efficient manner, resulting in an almost complete removal of the magnetization of the magnet blocks into a safe state. This method is seen as a more controlled alternative to the gas torch used in [10] and can in principle be applied on-site by

mounting several induction heater coils in a frame that is moved across the magnets of a direct drive wind turbine generator rotor. Secondly, it is easier to apply on-site compared to placing the entire generator rotor of D ~ 5-6 m and L ~ 2 m in a large furnace [10].

II. Materials and Methods

The induction heating experiments were conducted using a household induction heater, Tillreda from IKEA [11]. This device has a rated power of 2000 W and a cooking area with a diameter of 185 mm. The permanent magnet blocks used measured 10 cm x 7 cm x 2 cm with properties described below. These magnets were selected to represent wind turbine generator End-Of-Life magnets, but were obtained from a scrap yard, where the origin of the magnets could not be revealed. The magnets were received in the demagnetized state, they were cleaned by mechanically scraping off any traces of glue and then magnetized by applying a pulsed magnetic field of $\mu_0 H$ = 6 T along the short direction of the magnets. In the cross section revealed by cutting the magnets there was no sign of any protective metal coating on the magnet surface and it is believed that the magnets were only pacified before they were mounted in the application. The blocks were placed on the induction cooker with the largest surface in contact with the cooker. Due to the relatively small size of the magnets compared to the size of the induction plate, a block of aluminum was placed on a thin sheet of iron adjacent to the magnet block, in order to allow the heater to activate. The magnet and aluminum blocks were separated with a 2 mm thick ceramic plate. Type-*K* thermocouples were used to measure the temperature above and in one of the experiments also below the block, as shown in the sketch in Fig. 1. The top thermocouple was held in place by a disk-shaped piece of aluminum. Above the magnet block the magnetic field perpendicular to the induction plate was measured by a Hall sensor (GM 1-ST from Alpha Labs [12]) placed 70 mm above the magnet surface and 63 mm above the aluminum disc surface holding the top thermocouple. This height ensures that the Hall sensor does not experience elevated temperatures. The accuracy of the Hall sensor is ± 2% in the temperature interval -4 °C to 65 °C.

The operating frequency of the induction cooker was found, using an oscilloscope, to be f = 22 kHz. The skin depth δ to which the induction heating will penetrate into the magnet, is given by [13]

$$\delta = \sqrt{\frac{R}{\pi f \mu}} \quad (1)$$

Here R is the resistivity and μ is the permeability of the magnetic material, $\mu = \mu_r \mu_0$, where μ_r is the relative permeability and $\mu_0 = 1.257 \cdot 10^{-6}$ H/m is the vacuum permeability. With the parameters of the permanent magnet material from Table 1 a skin depth of δ = 4.4 mm is found.

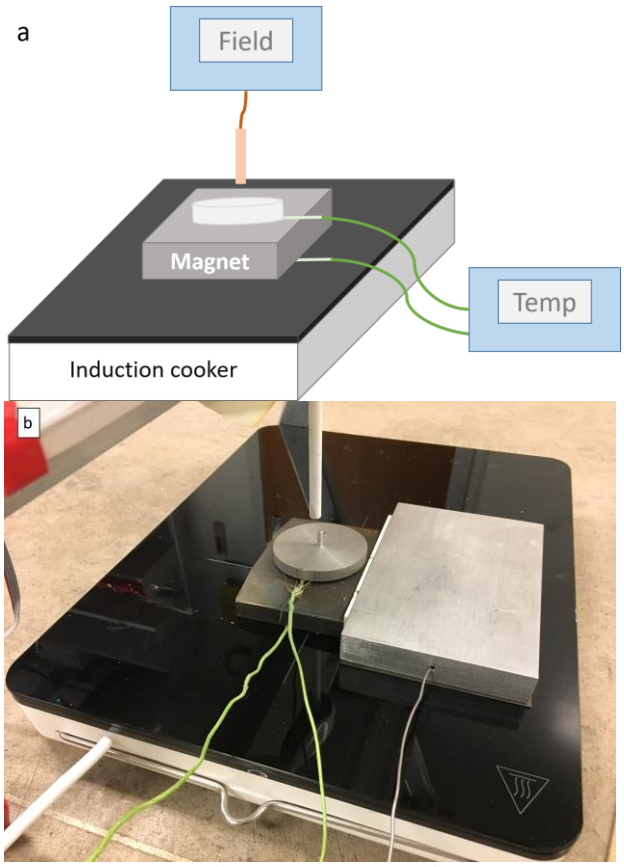

Fig. 1. Experimental setup for the demagnetizing of a large NdFeB magnet block. a) Sketch of position of thermocouples above and below the NdFeB magnet to measure the temperature and Hall probe placed above the magnet to measure the magnetic field during the demagnetization process. b) Picture of the setup used. The NdFeB magnet is seen on the left and a larger block of aluminum is placed to the right.

A. Characterization of permanent magnet materials

The properties of the permanent magnet blocks were characterized using the Cryogenic Limited CFMS 16 Tesla superconducting vibrating sample magnetometer equipped with a high temperature sample stage. A large magnet similar to the one in Fig. 1 was cut into cubic samples of about 2 x 2 x 3 mm using a diamond saw. A sample was mounted in a ceramic sample cup with the easy axis along the applied magnetic field. In Fig. 2a the magnetization, $\mu_0 M$, is plotted as a function of the internal field in the sample. The internal field $\mu_0 H$ is found by subtracting the demagnetization field, $\mu_0 H_d = N \cdot M$, from the applied field, $\mu_0 H_a$. N is the demagnetization constant of the measured sample, 0.240 in this case [14]. The measurements showed that at room temperature the remanence B_r was 1.17 T and the coercivity H_C was 1800 kA/m. Small jumps in the magnetization are observed just below zero internal field, at temperatures below 200 °C. These jumps are likely due to a soft magnetic phase on the surface of the small samples being measured, maybe due the cutting process [15]. A 40 µm surface imperfection of the sample would reduce the volume by more than 10 %.

This article has been accepted for publication in a future issue of this journal, but has not been fully edited. Content may change prior to final publication. Citation information: DOI 10.1109/TMAG.2020.3002098, IEEE Transactions on Magnetics

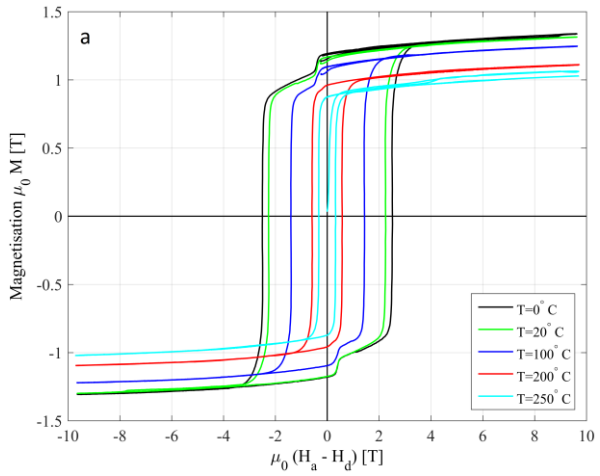

TABLE I
PARAMETERS USED FOR THE MODELLING OF THE PERMANENT MAGNET MATERIAL

Symbol	Quantity	Value
c_p	Specific heat	460 J·kg^{-1}·K^{-1}
k	Thermal conductivity	7.6 W·m^{-1}·K^{-1}
μ_r	Relative permeability	1.05
ρ	Density	7500 kg·m
R	Resistivity	180 · 10^{-8} Ωm

The values are taken from [16] and are assumed to be representative of the of the examined magnet blocks.

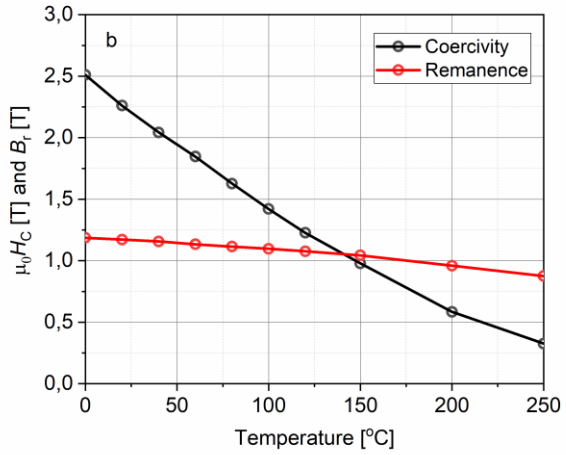

Fig. 2. Measured magnetization properties of the NdFeB magnet block. a) Temperature dependence of the magnetization versus internal magnetic field. b) Temperature dependence of the remanence, B_r, and the coercivity, H_C. Reproduced from [18].

The properties resemble those of the commercial N33UH from Arnold Magnetics [16] or Vacodym 677HR from Vacuumschmelze [17]. The temperature coefficients of the remanence and coercivity were found from a linear fit to the properties between the temperatures 20 °C and 100 °C. Values of -0.078 %/K and -0.46 %/K were found for the remanence and coercivity, respectively. These values are fairly close to the reported ones for the similar commercial magnet Vacodym 677HR from Vacuumschmelze, which has values of -0.085 %/K and -0.55 %/K, respectively, measured in the same temperature range.

The properties found above were applied in the following numerical modelling. Table 1 gives the remaining physical properties of the magnetic material.

B. *Numerical modelling*

A multi-physics model of the heating experiment was created in COMSOL Multiphysics, combining thermal and magnetic properties. A block of NdFeB with the size and shape given above, was modelled using the material properties given in Table 1. The Al cylinder on top was modelled using the properties of Al built into COMSOL. A control volume of air (500 x 500 x 600) mm^3 was modelled around the block.

The model solves the transient heat transfer equation to find the temperatures in the desired positions

$$\rho c_p \frac{\partial T}{\partial t} + \nabla \cdot (-k\nabla T) = Q \quad (2)$$

Where ρ is the density of the material, c_p is the specific heat and k is the thermal conductivity, all found in Table 1. Q is the sum of the volumetric heat inputs from the induction source and losses to the ambient.

The modelled time dependent temperatures are then used when modelling the magnetic properties using the temperature dependent remanence and coercivity found above.

Initially, everything starts at a constant temperature of 20 °C. Induction heating is applied in the volume of the magnet block closest to the induction heater, with a height of the skin depth δ. Convection and conduction losses are lumped into one term, applied to the full volume of the magnet block, and approximated to be linear in the temperature difference between ambient and the magnet block. Finally, radiation losses are modelled from all free surfaces as $-A\varepsilon\sigma(T^4 - T^4_{ambient})$, where A is the radiating surface area of the block, ε is the emissivity, assumed to be 0.95, and σ = 5.67·10^{-8} Wm^{-2}K^{-4} is the Stefan-Boltzmann constant.

III. INDUCTION HEATING RESULTS

A block of permanent magnet material was placed on the induction heater as described above and the heater was turned on. Fig. 3 shows the temperature measured by the thermocouple on top of the block of magnet increasing with time. Fig. 4 shows the measured magnetic field 70 mm above the block during the heating as a function of the temperature on top of the block. After reaching about 210 °C the magnetic field had almost been removed and the heater was turned off. The block of magnet was then allowed to cool back down to room temperature. After the magnet reached ambient temperature, the heater was turned on again, and the temperature of the block again increased, very similarly to the first heating sequence, as also shown in Fig 3. At 230 °C the heater was again turned off and the block was allowed to cool back down to room temperature. The small difference between

This article has been accepted for publication in a future issue of this journal, but has not been fully edited. Content may change prior to final publication. Citation information: DOI 10.1109/TMAG.2020.3002098, IEEE Transactions on Magnetics

the two heating curves is believed to be caused by a slight misalignment between the magnets and the induction coil in the two measurements.

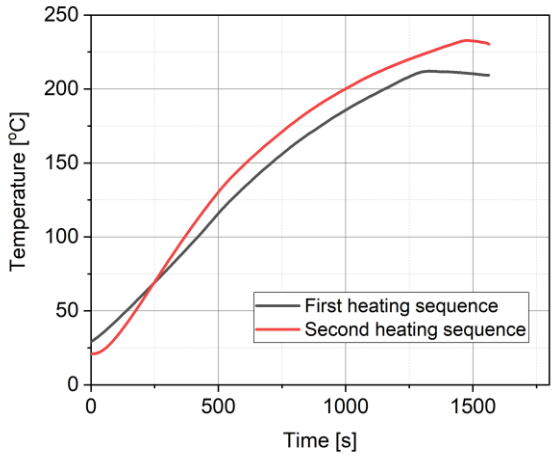

Fig. 3. Measured temperature at the top of the magnet block as a function of time after the heater is turned on. The second heating sequence follows after cooling the magnet block to room temperature.

In Fig. 4 it is observed how the magnetic field 70 mm above the magnet block remains almost constant at the low value of about 6.0 mT, until the temperature is increased above the maximum of the original heating. This further reduces the magnet field, resulting in a final value of 1.3 mT. A third heating sequence was performed up to a temperature of 275 °C, but no difference was observed compared to the second heating sequence, except for the fact that the magnetic field was further reduced to a value of 0.3 mT.

A second block of permanent magnet, with identical dimensions and magnetized in the same direction, was placed on the heater with one thermocouple located below and one above the block. The block was heated in intervals by repeatedly heating it to a certain temperature and letting it cool down for a period of time prior to the next heating sequence, as shown in Fig. 5a. A detail of this heating procedure is shown in Fig. 5b. Initially the block is cooling down from the previous heating, with both thermocouples showing similar values. At the time 2060 s the induction heater is turned on. Immediately the bottom thermocouple responds and starts heating, with the upper one exhibiting a lag of response. When the bottom one reaches 200 °C the heater is turned off. The bottom thermocouple immediately starts to cool down, while the response of the upper one is delayed due to the thermal resistance of the magnet block.

The magnetic field was recorded during the heating procedure as shown in Fig. 5a. The field is a little higher than in Fig. 4 due to the Hall sensor being placed at a distance of 42 mm this time. It is observed how the magnetic field drops during the heating periods, but recovers a little during the periods where the heater is turned off. This is due to equilibration of the temperature and decrease of the average temperature of the block.

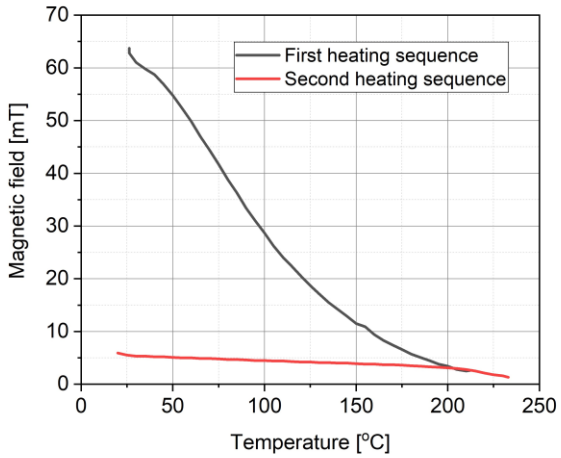

Fig. 4. Magnetic field measured 70 mm above the magnet block as a function of the temperature of the top surface of the magnet block. The magnet block was allowed to cool to room temperature after the first heating (black) before the second heating sequence was started (red). It is seen that the magnetic flux density is reduced by a factor of 10 between the first and second heating sequence resulting from the demagnetization of the magnet.

IV. Discussion

The transient properties during the heating and cooling in Fig. 5 can be used to make simple estimates of the heating power and heat losses in the system.

At around 3200 s both thermocouples have reached similar values and the temperature is decreasing at the same rate, with an average rate of -0.042 K/s at a temperature of 105 °C. Prior to heating the average slope of the cooling was -0.021 K/s at the time around 2000 s and temperature of 70 °C. The heat loss rate of the magnet block can be estimated as

$$P_{\text{loss}} = \dot{T} c_p m \tag{2}$$

Here $\dot{T}$ is the rate of temperature change, c_p is the specific heat from Table 1 and m is the magnet mass. Thus, the heat losses are -16.8 W and -8.4 W at 105 °C and 70 °C, respectively. Assuming a room temperature of about 20 °C, both cases give a heat loss of about P_{loss} = -0.2 W per degree above ambient (room temperature).

During the 220 s period of heating from 2060 s the bottom and top temperatures increase from both being 69 °C to being 201 °C and 103 °C, respectively. Assuming a linear temperature gradient inside the magnet this is equivalent to an average increase of ΔT_{avg} = 83 °C. The equivalent increase in thermal energy, E_{Therm}, is

$$E_{\text{Therm}} = c_p m \, \Delta T_{\text{avg}} \tag{3}$$

This gives a 33.1 kJ increase in the thermal energy. Assuming a constant heating during the time period Δt this is equivalent to a rate of power dissipation into the magnet of

$$P_{\text{induct}} = \frac{c_p m \, \Delta T_{\text{avg}}}{\Delta t} \tag{4}$$

This results in an average induction power of 150 W.

This article has been accepted for publication in a future issue of this journal, but has not been fully edited. Content may change prior to final publication. Citation information: DOI 10.1109/TMAG.2020.3002098, IEEE Transactions on Magnetics

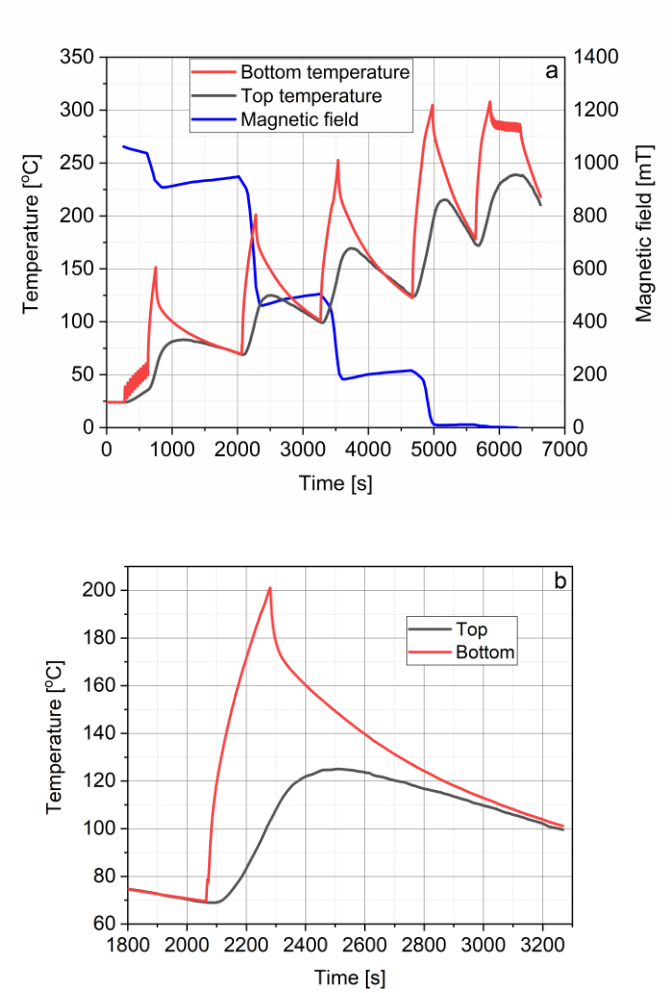

Fig. 5. Measured transient behavior of the temperature at the top and bottom of the magnet. a) Full measurement of temperatures above and below the magnet, as well as magnetic field 42 mm above the sample. The heating is turned on and off five times during the 6700 second measurement period. b) Zoom to a reduced temperature range between 1800 to 3300 second.

In Fig. 6a the numerical COMSOL model has been used to calculate the temperature on top of the block as a function of time, assuming a constant heating of the block of P_{induct} = 130 W and heat loss P_{loss} = -0.2 W·(T-$T_{ambient}$) as found above. It is observed that with this heating power the temperature reaches 200°C in approximately the same time as in Fig. 3. The heating power is lower than the one calculated from the data in Fig. 5. This may be due to a less central positioning of the magnet block in the first experiment. Fig. 6b shows the transient behavior of the temperatures above and below the magnet block. The heat source is turned on, now at 150 W, for 220 s, after which it is turned off. It is observed that the profile qualitatively is similar to that shown in Fig. 5b. In the experimental data the temperature increase is steeper and reaches a higher level. This may be due to a reduced thermal conductivity at the surface. In the model a value of 7.6 W/(m K) was used consistent with values from literature [16]. A lower value, especially at the surface, would allow the temperature to increase more, before allowing the heat to dissipate into the magnet. In addition, the heating in the skin depth is not uniform, but exponentially decaying from the surface. Thus, the heating at the bottom surface will be significantly higher than the average value used in the model.

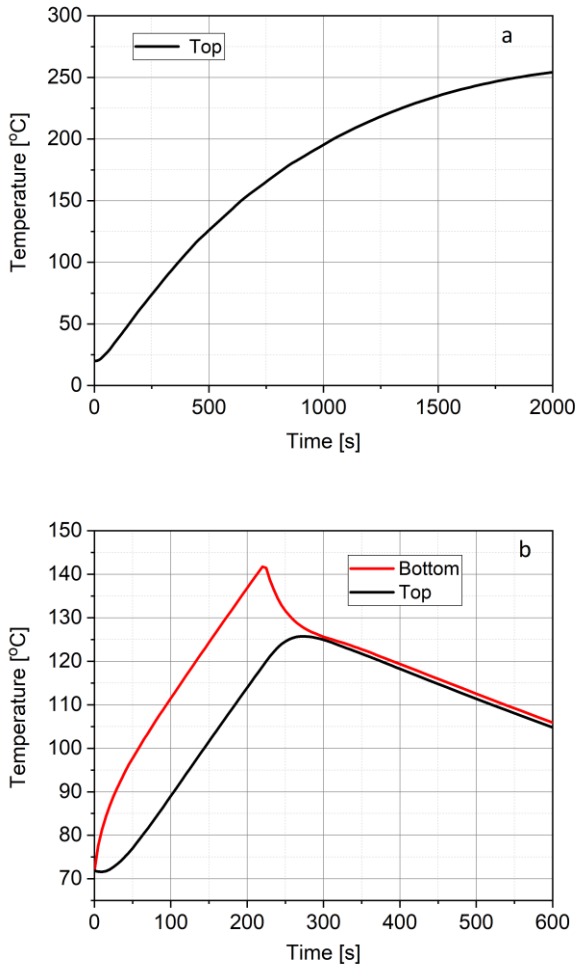

Fig. 6. Simulated magnet temperatures from the COMSOL model. a) The temperature at the top of the magnet block during constant heating of 130 W. b) Transient temperature behavior of the magnet block when a heating of 150 W is turned off after 220 seconds.

At zero applied magnetic field the internal field within a permanent magnet is due to the demagnetization field given by the magnetization and shape of the magnet. This so-called internal magnetic field defines the working point of the magnet in the second quadrant of the *B*-*H* curve. The internal field is temperature dependent through the temperature dependence of the remanence, discussed above. If the internal magnetic field approaches the coercivity of the permanent magnet, the magnet will experience an irreversible loss in magnetization. If it exceeds the coercivity, it will act to demagnetize the permanent magnet.

While often just characterized by a single demagnetization constant, the internal field is frequently reported as a single average value within a magnetic sample. In the numerical model, the internal field of the magnet block can be calculated locally. Fig. 7 shows the minimum, average and maximum internal field in the block as a function of its average internal temperature. The plot also shows the temperature dependence

of the coercivity found in the magnet characterization above, again plotted as a function of the average temperature. The lower part of the block will be a little hotter and the upper part will be a little colder, thus resulting in slightly lower and higher coercivities, respectively. Fig. 7 illustrates the loss of magnetization and thus measured magnetic field from the block during the induction heating, shown in Fig. 4. The inset in Fig. 7 shows how uniform the temperature is in a cross section of the magnet. The dominating temperature gradient is along the vertical direction.

The internal field curves in Fig. 7 depend strongly on the shape of the specific magnet block used. In the current experiment, a relatively flat block has been used, leading to a high demagnetization field within it. More cubically shaped blocks would result in a lower internal field, meaning a higher temperature is required to reach demagnetization.

It just requires more time to reach higher temperatures when heated with the induction cooker. Indeed, in a separate test heating of smaller cubic blocks with edge sizes of 1 cm up to 350 °C has been demonstrated. The remanence of the magnet block used here was 1.17 T. Magnet grades with higher remanence values up to and above 1.4 T are available and widely used in applications. The demagnetization field internally in the magnet is linear in the magnetization. Thus, the internal field of a 1.4 T magnet would be 20% higher than in a 1.17 T magnet block with the same shape.

Assuming that the two magnets have the same temperature dependent coercivity, this means that correspondingly less induction heating for demagnetization is required for future stronger magnets. It has been demonstrated that the quality of the magnet can vary through a block [19], so this could introduce a spread in the required temperature for demagnetization.

It has been shown that overheating the material to excessive temperatures eventually deteriorates the properties of the recycled magnets [20]. One concern of heating up the NdFeB material in air is that rare earth alloys are reacting with oxygen, whereby the magnetic phase is transformed into oxides. Even after numerous induction heating experiments there were no signs of color change of the surface of the magnets compared to the as received End-Of-Life state. The main parameter controlling the reaction rate of the magnets with air is the heating temperature. The induction heating method can demagnetize the large NdFeB magnets by heating the magnet to about 300 °C on the surface facing the induction heater, whereas a demagnetization using a gas torch might result in a much higher local surface temperature. Consequently, the controllability of the proposed method is considered superior. Here we have only discussed the demagnetization step of the recycling process. This is fundamental, but an often overlooked step towards the actual production of new magnets. With the material in a demagnetized state, several methods for magnet production are possible, see, e.g. refs. [7, 21].

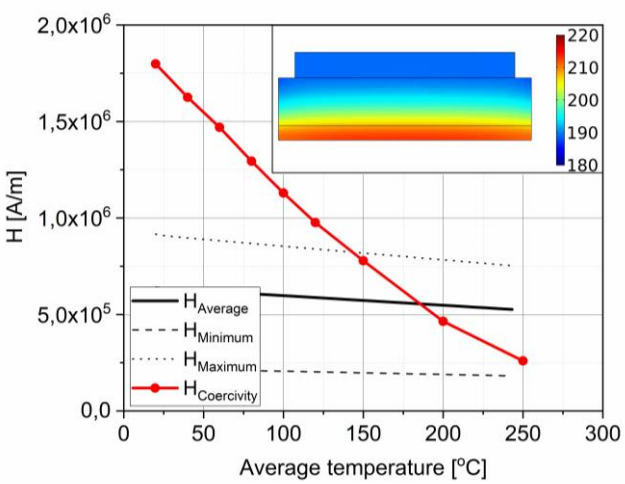

Fig. 7. Measured temperature dependent coercivity along with minimum, average and maximum magnetic field inside the large NdFeB magnet blocks as a function of the average temperature of the magnet as obtained from the finite element simulations. Inset: Cross section through the middle of the magnet block and aluminum disc showing the temperature in Celsius in the model after heating at 150 W for 500 s, corresponding to an average temperature of 205.5 °C.

V. Conclusions

It has been demonstrated how a simple 2 kW household induction cooker can be used to demagnetize 10 cm x 7 cm x 2 cm large End-of-Life NdFeB magnets to a level of 10 % of the initial magnetization in 30 minutes. A skin depth of 4.4 mm is estimated and the heating mechanism of the magnet seems to be the induced eddy currents. The temperature dependence of the remanence and coercivity of the magnets were determined and finite element simulations show that the demagnetization is accelerating in the temperature interval of 150 °C - 200 °C, where the internal demagnetization field becomes comparable and higher than the coercivity of the magnet. This temperature is considerably lower than the Curie Temperature of about 300 °C, illustrating that heating above the Curie temperature is not needed to obtain 90% demagnetization. Induction heating demagnetization of large NdFeB magnets provides a bulk heating method, and thus holds the potential of being faster and more efficient that the traditional methods. This is believed to be useful for demagnetizing large NdFeB magnet in the rotor structures of wind turbines generators that are being decommissioned and to provide a more well controlled process for the recycling of those magnets in the future.

Acknowledgment

A.B.A and M.A.E. acknowledge DTU Wind Energy for funding the internal ReMag project.

References

[1] Wind Europe, “Wind energy in Europe, Scenarios for 2030” report, Published 22 September 2017, www.windeurope.org

[2] Ørsted press release 13.04.2017 18:12 “DONG Energy awarded three German offshore wind projects”. Downloaded https://orsted.com/en/Company-Announcement-List/2017/04/1557851, July 2019.

[3] H. Polinder, J.A. Ferreira, B.B. Jensen, A.B. Abrahamsen, K. Atallah, and R.A. McMahon, “Trends in Wind Turbine Generator Systems”,

IEEE Journal of Emerging and Selected Topics in Power Electronics, Vol. 1, No. 3, September 2013, P. 174-185.

[4] H. Li, Z. Chen and H. Polinder, "Optimization of Multibrid Permanent-Magnet Wind Generator Systems", IEEE Transactions on Energy Conversion, Vol. 24, No. 1, March 2009, p. 82-92.

[5] A.B. Abrahamsen, D. Liu and H. Polinder, "Final assessment of superconducting (SC) and Pseudo Direct Drive (PDD) generator performance indicators (PI's)", Deliverable report D3.44 (2017) of the INNWIND.EU project. http://www.innwind.eu/publications/deliverable-reports

[6] M. Zakotnik, I.R. Harris and A.J. Williams, "Multiple recycling of NdFeB-type sintered magnets", Journal of Alloys and Compounds 469 (2009) 314–321

[7] Y. Yang, A. Walton, R. Sheridan, K. Güth, R. Gauß, O. Gutfleisch, M. Buchert, B.-M. Steenari, T. Van Gerven, P.T. Jones and K. Binnemans, "REE Recovery from End-of-Life NdFeB Permanent Magnet Scrap: A Critical Review", J. Sustain. Metall. (2017) 3:122–149

[8] I.C. Nlebedim and A.H. King, "Addressing Criticality in Rare Earth Elements via Permanent Magnets Recycling", JOM, Vol. 70, No. 2, (2018)

[9] T. Nemoto, Y. Tanaka, S. Tsujioka, Y. Eryu and T. Takada, "Resource Recycling for Sustainable Industrial Development", Hitachi Review Vol. 60 (2011), No. 6, 335-341

[10] A.M. Bundgaard and A. Remmen (Eds.), "Designing out waste", The Danish Environmental Protection Agency, ISBN: 978-87-93710-90-0, (2018).

[11] Ikea, Sweden, www.ikea.com

[12] AlphaLabs Inc., USA, www.alphalabinc.com

[13] B.I. Bleaney and B. Bleaney, "Electricity and Magnetism", Volume 1, Third edition, Oxford University Press, ISBN-0-19-851172-8 (1991).

[14] A. Aharoni, J. Appl. Phys. 83(6), 3432-3434 (1998)

[15] I. Petrov, D. Egorov, J. Link, R. Stern, S. Ruoho and J. Pyrhönen, "Hysteresis Losses in Different Types of Permanent Magnets Used in PMSMs", IEEE Trans. Industr. Electronics 64(3), 2502-2510 (2017)

[16] Arnold Magnetic Technologies Corp., USA. https://www.arnoldmagnetics.com/wp-content/uploads/2017/10/Catalog-151021.pdf

[17] Vacuumschmelze GmbH & Co. KG, Germany. https://www.vacuumschmelze.com/fileadmin/Medienbiliothek_2010/Downloads/DM/VACODYM-VACOMAX-PD002_2015_en.pdf

[18] M.A. Eder, "Investigate EBSD methods to establish relation between texture and magnetic properties of end of life and recycled rare earth – iron – boron permanent magnets", Master Thesis, DTU, 2018.

[19] A.J. Williams, R. Walls, B.E. Davies, J. Marchese and I.R. Harris, "A study of the thermal demagnetisation behaviour of Nd–Fe–B sintered magnets by a magnetic field mapping system", J. Magn. Magn. Mater. 242–245, 1378-1380 (2002).

[20] S. Högberg, F.B. Bendixen, N. Mijatovic, B.B. Jensen and J. Holbøll, "Influence of Demagnetization-Temperature on Magnetic Performance of Recycled Nd-Fe-B Magnets", Proceedings of the 2015 IEEE International Electric Machines and Drives Conference (IEMDC), 1242-1246 (2015)

[21] M. Xia, A.B. Abrahamsen, C.R.H. Bahl, B. Veluri, A.I. Søegaard, P. Bøjsøe, Poul, "Hydrogen Decrepitation Press-Less Process Recycling of NdFeB sintered magnets", J. Magn. Magn. Mater. 441, 55-61 (2017)